AIP | The Journal of Chemical Physics

Communication: On the stability of ice 0, ice i, and I h

D. Quigley, D. Alfè, and B. Slater

Citation: The Journal of Chemical Physics **141**, 161102 (2014); doi: 10.1063/1.4900772
View online: http://dx.doi.org/10.1063/1.4900772
View Table of Contents: http://scitation.aip.org/content/aip/journal/jcp/141/16?ver=pdfcov
Published by the AIP Publishing

Communication: On the stability of ice 0, ice i, and I_h

D. Quigley,[1,a)] D. Alfè,[2] and B. Slater[3]
[1]*Department of Physics and Centre for Scientific Computing, University of Warwick, Coventry CV4 7AL, United Kingdom*
[2]*Department of Earth Sciences and Department of Physics and Astronomy, University College London, Gower Street, London WC1E 6BT, United Kingdom*
[3]*Department of Chemistry, University College London, 20 Gordon Street, London WC1H 0AJ, United Kingdom*

(Received 18 September 2014; accepted 20 October 2014; published online 31 October 2014)

Using *ab initio* methods, we examine the stability of ice 0, a recently proposed tetragonal form of ice implicated in the homogeneous freezing of water [J. Russo, F. Romano, and H. Tanaka, Nat. Mater. **13**, 670 (2014)]. Vibrational frequencies are computed across the complete Brillouin Zone using Density Functional Theory (DFT), to confirm mechanical stability and quantify the free energy of ice 0 relative to ice I_h. The robustness of this result is tested via dispersion corrected semi-local and hybrid DFT, and Quantum Monte-Carlo calculation of lattice energies. Results indicate that popular molecular models only slightly overestimate the stability of ice zero. In addition, we study all possible realisations of proton disorder within the ice zero unit cell, and identify the ground state as ferroelectric. Comparisons are made to other low density metastable forms of ice, suggesting that the ice i structure [C. J. Fennel and J. D. Gezelter, J. Chem. Theory Comput. **1**, 662 (2005)] may be equally relevant to ice formation. [http://dx.doi.org/10.1063/1.4900772]

I. INTRODUCTION

Water ice is the most common mineral on earth and plays an important role in weather and climate, as well as countless natural processes and technological applications. Consequently, mapping the phase diagram of ice has received considerable attention by both experimental and theoretical methods, to better characterise this most fundamental of materials. A total of 15 ice phases[1] are known to be stable at various conditions of temperature and pressure and the last three phases: ice XIII,[2] XIV,[2] and XV,[3] have all been isolated within just the last few years. In addition, a number of stable[4–8,25] and hypothetical ice phases[9,10,29] have been predicted and characterised via computer simulation.

In a recent study, Russo, Romano, and Tanaka[11] presented evidence for a new metastable ice phase (termed ice 0) based entirely on simulations using coarse-grained[12] and atomistic[13] semi-empirical potentials. These simulations strongly imply a role for ice 0 in the nucleation and growth of ice I_h, a process fundamental to atmospheric science, cryogenics, geology, and astrophysics. As such, this new phase is potentially highly significant, and merits further attention with detailed *ab initio* methods, particularly as no experimental samples of ice 0 have yet been synthesised. The robustness of our calculated energetics is explicitly tested with higher level methods, specifically dispersion-corrected Density Functional Theory (DFT) and Quantum Monte-Carlo calculations, before making comparisons to other metastable phases ice phases proposed in the literature.

In this communication, we firmly establish the mechanical stability of the ice 0 structure using plane-wave DFT calculations, and characterise the possible proton orderings within this and other metastable ice phases. The robustness of our calculated energetics are explicitly tested with higher level methods, specifically dispersion-corrected DFT and Quantum Monte-Carlo calculations. The free energy relative to ice I_h is calculated via lattice dynamics and compared to the energetically similar ice i structure.[9]

II. RELATIVE ENERGETICS AND PROTON ORDERING

The ice 0 unit cell is analogous to the network proposed for semiconductors by Zhao *et al.*[14] It is tetragonal, with 12 molecules in the unit cell. Oxygen positions obey space group $P4_2/ncm$. A representation of the unit cell is shown in Figure 1.

We proceed to generate all possible proton positions which obey the Bernal-Fowler rules within the primitive unit cell. Using the method of graph invariants (see Refs. 4, 5, and 8) and using the GrEnum software,[15] we identify 52 structurally inequivalent proton configurations. Each of these has been relaxed to the corresponding local enthalpy minimum, without symmetry constraints. Calculations use the CASTEP plane-wave DFT code[16,17] with the Perdew, Burke and Ernzerhof (PBE)[18] generalised gradient approximation (GGA) functional and the in-built ultrasoft pseudopotentials.[19] Relaxation was performed using a two-point steepest descent algorithm.[20] The basis set was truncated at a plane wave energy of 490 eV with the Brillouin Zone sampled on a 6 × 6 × 4 *k* point grid. At this level, energy differences between configurations are converged to within 0.02 meV/molecule. We measure all energies per molecule and relative to that of ice XI[21] computed with the same basis set and *k* point density. PBESOL and PBE0 calculations were performed using CP2K[22] with a cutoff of 800 Ry and triple zeta quality basis

a)d.quigley@warwick.ac.uk

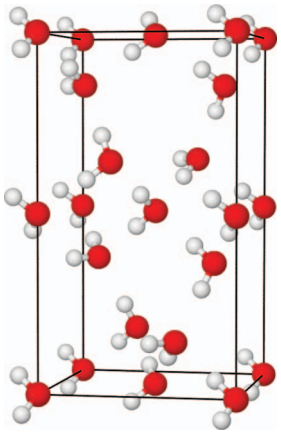

FIG. 1. Representation of the lowest energy (ferroelectric) proton ordering in ice 0 identified via PBE-DFT. Oxygen atoms are depicted in red and hydrogen in white.

set and we considered the effects of dispersion through the use of the Grimme's D3 correction term[23] in a supercell of dimensions $2 \times 2 \times 1$.

At the PBE level of theory, we identify the lowest energy proton configuration (Figure 1) as ferroelectric with $P2_1cn$ symmetry.[54] This lies 12.8 meV/molecule higher in energy than ice XI. The highest energy configuration lies an additional 4.4 meV/molecule higher. This is comparable to the energy range of proton configurations in ice I_h and I_c, for which various estimates in the range 3–5 meV/molecule exist in the literature,[24] and are found to be largely independent of the particular choice of functional.[25,26] These PBE data therefore indicate that ice 0 is less stable than ice I_h for all proton configurations, but only by virtue of an energy difference a few times larger in magnitude than the range resulting from proton disorder in either structure.

Structural parameters and energetics computed using DFT are compared to those obtained with the single-site mW model[12] and the TIP4P rigid-body atomistic model[27] in Table I.

As is evident from Table I, the relative stability of ice 0 to ice XI computed at the hybrid PBE0, PBE0+D3, and PBESOL+D3 levels of theory consistently reproduce the qualitative ordering predicted by mW, TIP4P, and PBE. Numerically, there is only a variation of 5.16 meV between all four functionals and notably, the influence of dispersion on stability is quite minor, as would be expected since the densities of ice 0 and XI are similar. The consistent energy difference given by GGA, hybrid and dispersion corrected versions of GGA and hybrid functional calculations give confidence that, in this instance, the numerical accuracy of all four approaches is expected to be reliable.

TABLE I. Summary of structural and energetic parameters obtained from relaxation of ice 0 (PBE lowest energy proton configuration). Energies are quoted per molecule and relative to the ice XI structure of Leadbetter *et al.*[21] DMC energies were computed at the PBE lattice parameters. Note that energies quoted in Ref. 28 are relative to an arbitrary configuration of ice I_h 7.7 meV higher in energy than ice XI within PBE-DFT.

	a (Å)	b (Å)	c (Å)	ΔE (meV)
TIP4P	6.04	6.04	10.94	7.21
mW	5.93	5.93	10.74	7.58
PBE	6.00	6.00	10.85	12.8
PBESOL+D3	5.70	5.71	10.30	15.3
PBE0+D3	6.03	5.94	10.67	12.5
PBE0	6.00	5.83	10.55	10.1
DMC	...	...	...	17 ± 5

III. COMPARISON TO OTHER METASTABLE ICES

The metastability of ice 0 at temperatures where ice can homogeneously nucleate is not unique. Ices II–IV are favoured over ice I_h only at high pressure, however, they are known to be remain mechanically stable under atmospheric pressure. To our knowledge, no study of ice nucleation has suggested that these phases are involved as metastable precursors to ice I_h, and their high energy relative to ice I makes this rather unlikely. A number of additional ice structures, with no region of thermodynamic stability have been proposed via computer simulation.

Svishchev and Kusalik[10] identified an orthorhombic phase of ice with $Pnc2$ symmetry by conducting electrofreezing simulations of the TIP4P[27] water model. As previously reported[28] the static lattice energy of this structure computed via PBE-DFT under atmospheric pressure lies intermediate between ices II and III and is equally unlikely to be involved in nucleation of ice I_h. Relative to the PBE energy, calculations using TIP4P increase the stability relative to ice I_h by 37.8 meV/molecule. We find this structure to be mechanically unstable within the single-site mW model,[12] resulting in relaxation to ice III. By analogy with silica, Tribello *et al.*[29] have proposed "quartz ice" with $P3_121$ symmetry. In common with the Svishchev and Kusalik[10] structure, this is unstable within the mW model, but can be simulated with TIP4P. This predicts a similar reduction in energy relative to ice I_h (34.5 meV/molecule) when compared to the PBE prediction.

Fennell and Gezelter[9] proposed a further phase, termed ice i. This low density P_4/mmm phase was identified as possessing *greater* stability that ice I_h for a number of semi-empirical potentials when using an approximate treatment of long range electrostatics, suggesting it could be energetically competitive in more accurate calculations. This structure is mechanically stable within the mW model, lying 21.4 meV/molecule higher in energy that ice I_h. TIP4P calculations with an accurate treatment of long range electrostatics reduce this penalty to 12.0 meV/molecule. Despite these small energy differences, ice i has not been observed in simulations of ice nucleation and growth[30–35] that use these models.

For each of these phases, we have enumerated all symmetry non-equivalent proton configurations which can be realised within the primitive unit cell and computed their energies using identical basis set and BZ sampling to the ice I_h and ice 0 results reported in Sec. II. Results are reported in Table II.

Although ice 0 is clearly the most stable of these four phases, ice i is sufficiently competitive that their respective

TABLE II. Calculated lower (ΔE_l) and upper (ΔE_u) PBE energy difference to ice XI (per molecule) across all proton configurations in metastable ice phases previously proposed via computer simulation. The densities presented are those of the relaxed unit cell under zero pressure, and are consistent across all proton configurations to the precision quoted.

	ΔE_l (meV)	ΔE_u (meV)	ρ (kg m^{-3})
Ice 0[11]	12.8	17.1	921
Ice i[9]	17.3	24.7	903
Quartz ice[29]	46.6	52.8	1096
Electrofrozen ice[10]	69.0	77.1	1062

range of energies resulting from proton disorder are close to overlapping. Indeed the energy gap between them is very much smaller than the variation of ice 0 energies between functionals in Table I, suggesting that the two structures cannot be resolved as energetically distinct at this level of theory. Conde *et al.*[36] previously computed the energy of a single proton realisation of ice i to be only 12 meV/molecule higher in energy than ice XI. This calculation used anti-ferroelectric ice XI[37] rather than the ferroelectric form used here, and the PW91 functional. To compare this figure to those in Table II, we have computed the PW91[38] energy difference between the anti-ferroelectric and ferroelectric ice XI structures to be 4.5 meV/molecule. The remaining difference to the range in Table II can be attributed to variations between functionals, or the use of a larger ice i supercell in Ref. 36 which may have contained a particularly stable proton configuration not sampled in our smaller unit cells. In either case it is clear that ice 0 and ice i cannot easily be separated on DFT lattice energies alone.

IV. QUANTUM MONTE CARLO

To assess the veracity of the DFT-computed energies in Tables I and II, we turn to a benchmark method. Quantum Monte Carlo calculations have been performed with the CASINO code[47] within the fixed-node approximation and Dirac-Fock pseudo potentials.[48] The core radii of the oxygen and the hydrogen pseudo potentials were 0.4 Å and 0.26 Å, respectively. The trial wavefunctions were of the Slater-Jastrow type, with a single Slater determinant. The single particle orbitals were obtained from DFT-LDA plane-wave calculations using the pwscf package,[49] using a plane-wave cutoff of 300 Ry, and were re-expanded in B-splines.[50] In diffusion Monte Carlo (DMC) we used the locality approximation[51] and a time step of 0.002 a.u., which were shown to give energy differences between ices II and VIII converged to within ∼5 meV/molecule.[53] The DMC calculations were performed on a 2 × 2 × 2 supercell of the lowest energy (with PBE-DFT) proton configuration, containing 96 molecules, and using the Model Periodic Coulomb (MPC) technique to treat the electron-electron interactions. This helps to significantly reduce DMC size errors.[52] Size tests performed on the VIII and the II structures[53] showed that, with cells including 96 molecules or more, finite size error are reduced to less than 5 meV/molecule.

We performed a single point calculation, using the lattice parameters $a = 5.99807$, $b = 5.99478$, $c = 10.8367$, which are close to the PBE equilibrium volume. The DMC energy of the ice 0 structure is calculated to be 17 ± 5 meV/molecule higher than ice I_h. A similar computation was performed for the lowest energy proton configuration of ice i, using 96 molecules in a 2 × 2 × 3 supercell, yielding an energy 24 ± 5 meV higher than the same ice I_h reference structure (equal in energy to ice XI within this statistical accuracy). As an aside, we note the ice 0 energy is essentially degenerate with that of an empty sI hydrate 15 ± 5 meV/molecule[39] at this level of theory.

Comparing to the PBE-DFT energies in Table II, these DMC energies are shifted upward by 4–7 meV. Within the context of a 5 meV statistical error and a similar variation between DFT functionals in Table I, we conclude that DFT and DMC produce consistent lattice energies within their respective uncertainties, and that one cannot confidently separate ice 0 and ice i on the basis of static lattice energies alone.

V. LATTICE DYNAMICS

To establish the mechanical stability of ice zero and assess the vibrational contribution to its free energy, we have computed its phonon spectrum. Calculations were performed using two representative proton configurations with zero net dipole. The first of these retains some symmetry ($P2_1$), and the second belongs to $P1$ only. Similar calculations were performed on the antiferroelectric $P4_2/mnm$ ground state of ice i,[54] and a representative eight-molecule cell of ice I_h (dimensions 4.41 × 7.20 × 7.63 Å).

Phonon calculations were performed within the density functional perturbation theory (DFPT) framework as implemented in the CASTEP code[40] and used norm-conserving pseudopotentials from the Bennett and Rappe pseudopotential library[41] requiring a plane wave energy of 750 eV to achieve a similar level of convergence to the above ultrasoft calculations. Structural relaxation reveals the $P2_1$ ice 0 configuration to be 1.2 meV/molecule higher in energy than $P1$, which in turn is 7.8 meV/molecule higher in energy than the ice I configuration.

Computed Helmholtz free energies were converged explicitly with respect to sampling of the vibrational Brillouin Zone (BZ). Ice 0 results are quoted for a γ-centred 3 × 3 × 2 grid. Results changed by no more than 0.3 meV/molecule upon increasing to 4 × 4 × 3 or 5 × 5 × 4. Equivalent convergence was obtained with the ice i structure by sampling on a 3 × 3 × 5 grid, and ice I_h on a 5 × 5 × 3 grid.

The phonon dispersion relation of the $P2_1$ ice 0 structure obtained by Fourier interpolation along high symmetry directions is plotted in Figure 2. The lack of negative frequencies establishes ice 0 as mechanically stable. A similar exercise confirms the mechanical stability of ice i, which we do not believe has been previously reported in *ab initio* calculations. The computed Helmholtz free energies of these structures are presented in Table III for a temperature of 250 K – the approximate melting temperature of ice 0. The temperature dependence in this quantity is weak, varying by less than the BZ-sampling error down to a temperature of 180 K, the range

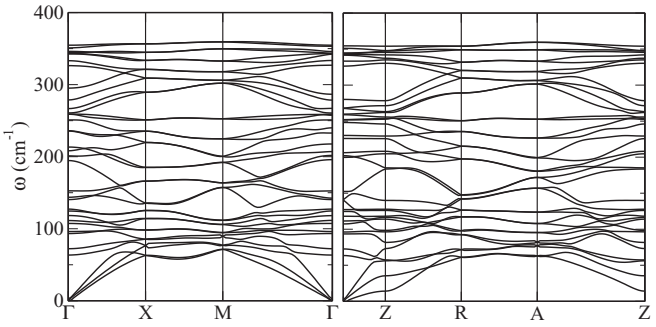

FIG. 2. Low frequency phonon dispersion plot for the ice 0 $P2_1$ configuration computed using PBE-DFT. Higher frequency libration, bending, and stretching modes are omitted for brevity.

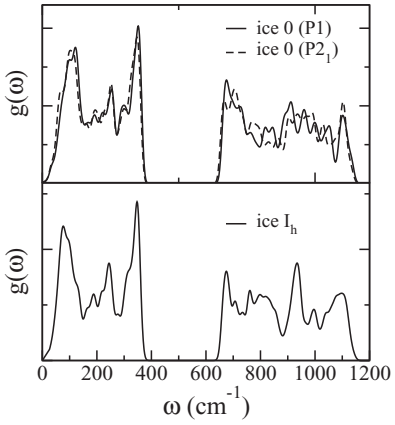

FIG. 3. Phonon density of states $g(\omega)$ for two ice 0 proton configurations (top) and a single proton configuration of ice I_h (bottom). Higher frequency bond bending and stretching modes are omitted for clarity.

over which ice 0 may play a role in the homogeneous nucleation of ice I_h.

The vibrational contribution to the free energy difference between ice 0 and ice I_h is similar in magnitude to the lattice energy difference between proton orderings. This is confirmed by similarity in the phonon density of states (DOS) of the two structures, plotted in Figure 3, suggesting that vibrations can be reasonably neglected when comparing the gross stability of these structures.

Table III also indicates that the most stable ice i proton configuration lies *between* two ice 0 configurations in Helmholtz free energy. The incorporation of vibrational effects does not therefore provide any basis to thermodynamically separate ice 0 from ice i.

VI. DISCUSSION

It is instructive to consider the data in Table II in the context of classical nucleation theory (CNT). Neglecting kinetic considerations, in order for initial nuclei to adopt a metastable crystal structure, the crystal-liquid interfacial free energy γ_{sl} of that phase must be lower than the stable phase, in this case ice I_h. Quantification of γ_{sl} remains a challenge, and we are not aware of a study which has achieved this for anything other than simple atomistic models. Evaluating this quantity at the *ab initio* level is currently impossible.

However, we can use CNT to estimate how much γ_{sl} for the metastable phase must be reduced relative to that of ice I_h in order to play such a role in the homogeneous nucleation of ice. By using thermodynamic data established as consistent with direct measurements of critical nuclear size data[42] we compute CNT barrier heights to homogeneous nucleation of ice I_h, established as consistent with molecular simulations at moderate supercooling.[43]

Equating these to the barrier height for nucleation of ice 0 and inserting the PBE thermodynamic data computed in Sec. V, we establish that the ice 0 γ_{sl} need only be approximately 5% lower than in ice I_h in order for ice zero to nucleate preferentially at 200 K, decreasing to 10% lower at 240 K. This requirement is relaxed slightly to 3% (200 K) and 8% (240 K) in the TIP4P and mW models. Similar figures are obtained for ice i.

Russo, Romano, and Tanaka[11] have noted that the ice 0 melting curve, and hence its stability relative to liquid water, mirrors the homogeneous nucleation line of ice I_h. The *ab initio* data reported here indicate that ice i has a similar enthalpy and volume, suggesting via the Clausius-Clapeyron equation that its stability will continue to track that of ice 0 at increasing pressure. However, since ice i is not observed to form in nucleation simulations, one might expect to find a higher γ_{sl} for that phase.

Variation in γ_{sl} between the basal, prism, and $\{11\bar{2}0\}$ faces of TIP4P ice I_h has been calculated to be 4–6%.[44,45] A similar magnitude of variation between ice phases of varying density is certainly plausible. We defer explicit calculation of interfacial free energies to future work, however one might expect the interfacial energy of *both* ice 0 and ice i to be lower than ice I_h due to their lower density and cohesive energy. Both ice 0 and ice i are significantly more stable (∼40 meV/molecule at the PBESOL-D3 level, configuration taken from Ref. 46) than low density amorphous ice, which is of comparable density to ice 0 and ice i, suggesting that ordered structures may be more effective at mediating the nucleation of ice I_h.

TABLE III. Static lattice energy difference (ΔE), zero point energy difference, and Gibbs free energy difference between two ice 0 proton configurations, the lowest energy ice i proton configuration, and an arbitrarily selected proton configuration of ice I_h. All energies are quoted in meV/molecule.

	ΔE (meV)	ΔE_{zp} (meV)	ΔG (meV) (250 K)
Ice 0 $P2_1$	9.0	0.6	10.3
Ice 0 $P1$	7.8	1.7	11.6
Ice i $P4_2/mnm$	9.9	1.0	10.7

ACKNOWLEDGMENTS

D.Q. is supported by EPSRC Grant No. EP/H00341X/1. This work used computing resources provided by the Centre for Scientific Computing at the University of Warwick. Via our membership (B.S.) of the UK's HPC Materials Chemistry Consortium, which is funded by EPSRC (EP/L000202), this

work made use of the facilities of HECToR and ARCHER, the UK's national high-performance computing service, which is funded by the Office of Science and Technology through EPSRC's High End Computing Programme. This research used resources of the Oak Ridge Leadership Computing Facility located in the Oak Ridge National Laboratory, which is supported by the Office of Science of the Department of Energy under Contract No. DE-AC05-00OR22725.

[1]C. G. Salzmann, P. G. Radaelli, B. Slater, and J. L. Finney, Phys. Chem. Chem. Phys. **13**, 18468 (2011).
[2]C. G. Salzmann, P. G. Radaelli, A. Hallbrucker, E. Mayer, and J. L. Finney, Science **311**, 1758 (2006).
[3]C. Salzmann, P. Radaelli, E. Mayer, and J. Finney, Phys. Rev. Lett. **103**, 105701 (2009).
[4]S. Singer, J.-L. Kuo, T. Hirsch, C. Knight, L. Ojamäe, and M. Klein, Phys. Rev. Lett. **94**, 135701 (2005).
[5]C. Knight and S. J. Singer, J. Phys. Chem. B **109**, 21040 (2005).
[6]J.-L. Kuo, Phys. Chem. Chem. Phys. **5**, 3733 (2005).
[7]J.-L. Kuo and W. F. Kuhs, J. Phys. Chem. B **110**, 3697 (2006).
[8]S. Singer and C. Knight, J. Chem. Phys. **129**, 164513 (2008).
[9]C. J. Fennell and J. D. Gezelter, J. Chem. Theory Comput. **1**, 662 (2005).
[10]I. M. Svishchev and P. G. Kusalik, Phys. Rev. B **53**, R8815 (1996).
[11]J. Russo, F. Romano, and H. Tanaka, Nat. Mater. **13**, 670 (2014).
[12]V. Molinero and E. B. Moore, J. Phys. Chem. B **113**, 4008 (2009).
[13]J. Abascal and C. Vega, J. Chem. Phys. **123**, 234505 (2005).
[14]Z. Zhao, F. Tian, X. Dong, Q. Li, Q. Wang, H. Wang, X. Zhong, B. Xu, D. Yu, J. He, H.-T. Wang, Y. Ma, and Y. Tian, J. Am. Chem. Soc. **134**, 12362 (2012).
[15]"GrEnum," see https://chemistry.osu.edu/~singer/GrEnum.html for a description of this software and the algorithms therein.
[16]S. J. Clark, M. D. Segall, C. J. Pickard, P. J. Hasnip, M. J. Probert, K. Refson, and M. C. Payne, Z. Kristall. **220**, 567 (2005).
[17]M. C. Payne, M. P. Teter, D. C. Allan, T. Arias, and J. D. Joannopoulos, Rev. Mod. Phys. **64**, 1045 (1992).
[18]J. P. Perdew, K. Burke, and M. Ernzerhof, Phys. Rev. Lett. **77**, 3865 (1996).
[19]D. Vanderbilt, Phys. Rev. B **41**, 7892 (1990).
[20]J. Barzilai and J. M. Borwein, IMA J. Numer. Anal. **8**, 141 (1988).
[21]A. J. Leadbetter, R. C. Ward, J. W. Clark, P. A. Tucker, T. Matsuo, and H. Suga, J. Chem. Phys. **82**, 424 (1985).
[22]J. VandeVondele, M. Krack, F. Mohamed, M. Parrinello, T. Chassaing, and J. Hutter, Comp. Phys. Commun. **167**, 103 (2005).
[23]S. Grimme, J. Antony, S. Ehrlich, and H. Krieg, J. Chem. Phys. **132**, 154104 (2010).
[24]Z. Raza, D. Alfè, C. G. Salzmann, J. Klimes, A. Michaelides, and B. Slater, Phys. Chem. Chem. Phys. **13**, 19788 (2011).
[25]G. A. Tribello, B. Slater, and C. G. Salzmann, J. Am. Chem. Soc. **128**, 12594 (2006).
[26]F. Labat, C. Pouchan, C. Adamo, and G. E. Scuseria, J. Comp. Chem. **32**, 2177 (2011).
[27]W. L. Jorgensen, J. Chandrasekhar, J. D. Madura, R. W. Impey, and M. L. Klein, J. Chem. Phys. **79**, 926 (1983).
[28]B. Slater and D. Quigley, Nat. Mater. **13**, 733 (2014).
[29]G. A. Tribello, B. Slater, M. A. Zwijnenburg, and R. G. Bell, Phys. Chem. Chem. Phys. **12**, 8597 (2010).
[30]R. Radhakrishnan and B. Trout, J. Am. Chem. Soc. **125**, 7743 (2003).
[31]D. Quigley and P. M. Rodger, J. Chem. Phys. **128**, 154518 (2008).
[32]A. V. Brukhno, J. Anwar, R. Davidchack, and R. Handel, J. Phys.: Condens. Matter **20**, 494243 (2008).
[33]T. Li, D. Donadio, G. Russo, and G. Galli, Phys. Chem. Chem. Phys. **13**, 19807 (2011).
[34]A. Reinhardt and J. P. K. Doye, J. Chem. Phys. **136**, 054501 (2012).
[35]A. Reinhardt and J. P. K. Doye, J. Chem. Phys. **139**, 096102 (2013).
[36]M. M. Conde, C. Vega, G. A. Tribello, and B. Slater, J. Chem. Phys. **131**, 034510 (2009).
[37]E. R. Davidson and K. Morokuma, J. Chem. Phys. **81**, 3741 (1984).
[38]J. P. Perdew and Y. Wang, Phys. Rev. B **45**, 13244 (1992).
[39]S. J. Cox, M. D. Towler, D. Alfè, and A. Michaelides, J. Chem. Phys. **140**, 174703 (2014).
[40]K. Refson, P. R. Tulip, and S. J. Clark, Phys. Rev. B **73**, 155114 (2006).
[41]J. W. Bennett and A. M. Rappe, see http://www.sas.upenn.edu/rappegroup/research/pseudo-potential-gga.html for pseudopotential files and generation information.
[42]J. Liu, C. E. Nicholson, and S. J. Cooper, Langmuir **23**, 7286 (2007).
[43]E. Sanz, C. Vega, J. R. Espinosa, R. Caballero-Bernal, J. L. F. Abascal, and C. Valeriani, J. Am. Chem. Soc. **135**, 15008 (2013).
[44]R. Handel, R. L. Davidchack, J. Anwar, and A. Brukhno, Phys. Rev. Lett. **100**, 036104 (2008).
[45]J. Benet, L. G. MacDowell, and E. Sanz, Phys. Chem. Chem. Phys. **16**, 22159 (2014).
[46]R. Martok, D. Donadio, and M. Parrinello, J. Chem. Phys. **122**, 134501 (2005).
[47]R. J. Needs, M. D. Towler, N. D. Drummond, and P. L. Ros, J. Phys.: Condens. Matter **22**, 023201 (2010).
[48]J. R. Trail and R. J. Needs, J. Chem. Phys. **122**, 174109 (2005).
[49]See www.quantum-espresso.org for source code, pseudopotential files and documentation.
[50]D. Alfè and M. Gillan, Phys. Rev. B: Condens. Matter Mater. Phys. **70**, 161101 (2004).
[51]L. Mitáš, E. L. Shirley, and D. M. Ceperley, J. Chem. Phys. **95**, 3467–3475 (1991).
[52]L. M. Fraser, W. M. C. Foulkes, G. Rajagopal, R. J. Needs, S. D. Kenny, and A. J. Williamson, Phys. Rev. B: Condens. Matter **53**, 1814–1832 (1996).
[53]B. Santra, J. Klimes, D. Alfè, A. Tkatchenko, B. Slater, A. Michaelides, R. Car, and M. Scheffler, Phys. Rev. Lett. **107**, 185701 1-5 (2011).
[54]See supplementary material at http://dx.doi.org/10.1063/1.4900772 for complete coordinate listing of the ground state proton configurations in ice 0 and ice i, and a visualisation of the latter.